analytical chemistry

Article

pubs.acs.org/ac

Luminescent Iridium(III) Complex Labeled DNA for Graphene Oxide-Based Biosensors

Qingcheng Zhao,[†,§] Yuyang Zhou,[‡,§] Yingying Li,[†] Wei Gu,[†] Qi Zhang,[*,†] and Jian Liu[*,†]

[†]Jiangsu Key Laboratory for Carbon-Based Functional Materials and Devices, Institute of Functional Nano and Soft Materials (FUNSOM), Collaborative Innovation Center of Suzhou Nano Science and Technology, Soochow University, Suzhou, Jiangsu 215123, China

[‡]Jiangsu Key Laboratory of Environmental Functional Materials, School of Chemistry, Biology and Material Engineering, Suzhou University of Science and Technology, Suzhou 215009, China

Supporting Information

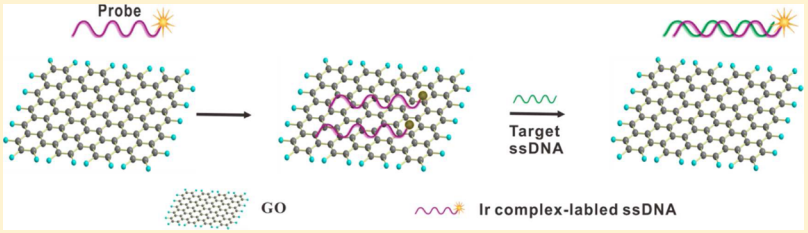

ABSTRACT: There has been growing interest in utilizing highly photostable iridium(III) complexes as new luminescent probes for biotechnology and life science. Herein, iridium(III) complex with carboxyl group was synthesized and activated with *N*-hydroxysuccinimide, followed by tagging to the amino terminate of single-stranded DNA (ssDNA). The Ir-ssDNA probe was further combined with graphene oxide (GO) nanosheets to develop a GO-based biosensor for target ssDNA detection. The quenching efficiency of GO, and the photostability of iridium(III) complex and GO-Ir-ssDNA biosensor, were also investigated. On the basis of the high luminescence quenching efficiency of GO toward iridium(III) complex, the GO-Ir-ssDNA biosensor exhibited minimal background signals, while strong emission was observed when Ir-ssDNA desorbed from GO nanosheets and formed a double helix with the specific target, leading to a high signal-to-background ratio. Moreover, it was found that luminescent intensities of iridium(III) complex and GO-Ir-ssDNA biosensor were around 15 and 3 times higher than those of the traditional carboxyl fluorescein (FAM) dye and the GO-FAM-ssDNA biosensor after UV irradiation, respectively. Our study suggested the sensitive and selective Ir-ssDNA probe was suitable for the development of highly photostable GO-based detection platforms, showing promise for application beyond the OLED (organic light emitting diode) area.

Sensitive and selective detection of biomolecules is very important and urgently needed in the field of molecular diagnostics, drug discovery, and food safety. To develop rapid, trustworthy, easy to use, and cost-effective biosensors for biomolecule detection,[1] nanomaterials are employed to design novel biosensors due to their unique optical, electronic, and magnetic properties. Hence, much recent work has focused on the design of nanoprobes by combining nanomaterials with biomolecular recognition units.[2] For instance, gold nanoparticles (AuNPs),[3] quantum dots (QDs),[4] carbon nanotubes (CNTs),[5] and transition metal dichalcogenides (WS_2)[6] are investigated, which offer desirable and unmatched characteristics for biological detection.

Very recently, graphene-based fluorescent biosensors offer numerous opportunities to develop new measurement methodology for nucleic acids,[7] proteins,[8] ions,[9] and small molecules[10,11] detection. Graphene, along with graphene oxide (GO), can serve as a good carrier for biomolecules due to its large specific surface area (theoretical 2630 m^2/g) and sp^2-bonded carbon structure.[12,13] Graphene can noncovalently adsorb fluorophore-labeled single-stranded DNA (ssDNA) by $\pi-\pi$ stacking between nucleotide bases and carbon plane, and quench the fluorescence according to the Förster resonance energy transfer (FRET)[14] from the fluorophore to the carbon plane. In contrast, graphene can hardly interact with rigid duplex formation. In the case of the target present, the formation of duplex structures between the desorbed fluorophore-labeled ssDNA and the target can restore the fluorescence emission of the dye, providing a fluorescent-based quantitative approach for DNA/RNA and protein analysis. In addition, graphene can protect DNA/RNA against enzymatic cleavage[15] and promote the intracellular stability of DNA/RNA,[16] as compared to free DNA/RNA probes.

In the graphene-based biosensors, the physicochemical properties of fluorophore play a crucial role in the quenching and recovery cycle of fluorescence. The dye with conjugated-π bond can form a strong interaction with graphene, generating an effective FRET from fluorophore to carbon plane. Lu et al.[17]

Received: November 15, 2015
Accepted: January 12, 2016
Published: January 12, 2016

DOI: 10.1021/acs.analchem.5b04324
Anal. Chem. 2016, 88, 1892−1899

designed a carboxyl fluorescein (FAM)-labeled ssDNA probe, of which GO could bind and quench it. In the presence of the target, the FAM-labeled ssDNA can release from GO surface and combine with target DNA to form a double-stranded DNA (dsDNA) structure, resulting in fluorescence recovery. Fan and co-workers[18] designed and prepared three different DNA probes conjugated with three different fluorescent dyes (FAM, 6-carboxyl-X-rhodamine, and cyanine 5) complementary for three kinds of target DNA, which allowed the sensitive detection of specific target DNA simultaneously. However, the photostability of these traditional dyes was quite weak. A light-shielding device is usually necessary to avoid dye decay during chemical and physical treatments, which is inconvenient and hinders their applications in optical detection. Iridium complexes, the metal-based emissive probes, can be adopted as interesting alternatives,[19] because they exhibit advantageous photophysical properties for bioimaging[20] and biosensing,[21−23] such as enhanced photostability,[24] and large Stokes shifts.[25] This highly photostable characteristic of Ir complex makes it a promising platform for application in optical detection.[26]

Taking advantage of the unique GO/ssDNA interaction and high photostability of Ir complexes, we synthesized an Ir complex-labeled ssDNA (Ir-ssDNA) probe and further combined with GO to fabricate GO-Ir-ssDNA biosensor for target DNA detection. We demonstrated that the fluorescence of Ir-ssDNA would be quenched by graphene plane in the GO-Ir-ssDNA system and effective response to target molecules. The interaction between Ir complex and GO, photostability of Ir complex and Ir-ssDNA, and specificity of target DNA detection were investigated. This proof of concept might provide a robust and highly photostable approach for biomolecule detection, promising Ir complex in application beyond the OLED (organic light emitting diode) area.

EXPERIMENTAL SECTION

Chemicals and Materials. $IrCl_3·3H_2O$, *N*,*N*-dimethylformamide (DMF), 4-(4′-methyl-[2,2′-bipyridin]-4-yl)butanoic acid (bpy-COOH), 2-phenylpyridine (ppy), *O*-benzotriazole-*N*,*N*,*N*′,*N*′-tetramethyl-uronium-hexafluorophosphate (HBTU), carboxyl fluorescein (FAM), and *N*-hydroxysuccinimide (NHS) were purchased from Sigma-Aldrich. 2-Ethoxyethanol, ethanol, *n*-hexane dichloromethane, and methanol were obtained from Sinopharm Chemical Reagent Co., Ltd.

Apparatus. ^{1}H NMR spectra were recorded with a Varian spectrometer at 400 MHz. TOF-MS were measured on New ultrafle Xtreme MALDI TOF/TOF. UV−vis absorption spectra were characterized using a PerkinElmer lambda 750 UV−vis near-infrared spectrophotometer. Atomic force microscopy (AFM) image was acquired with a Multi-Mode V AFM (Veeco). Fluorescent emission spectra were performed using a HORIBA JOBTN YVON FLUOROMAX-4 spectrofluorimeter. All experiments were carried out at room temperature. The luminescence intensity was monitored in a 350 μL quartz cuvette sample cell by exciting the sample at 360 nm and measuring the emission at 570 nm. The slits for excitation and emission were both set at 5 nm.

Synthesis of Ir Complexes. The iridium(III) complexes were synthesized according to previously reported methods.[27,28] The synthetic route was divided into three steps: Step 1, a solution of $IrCl_3·3H_2O$ (1 equiv) and 2-phenylpyridine (2 equiv) in the mixture of 2-ethoxyethanol/H_2O (v:v = 3:1) was refluxed for 24 h under argon atmosphere. After being cooled to room temperature, the solution was filtrated, and the precipitate was successively washed with water, ethanol, and *n*-hexane. The dichlorobridged iridium(III) dimer was obtained after drying.

Step 2, a solution of 2.2 equiv of 4-(4′-methyl-[2,2′-bipyridin]-4-yl)butanoic acid (bpy-COOH) and 1 equiv of dichlorobridged iridium(III) dimer in the mixture of CH_3OH/CH_2Cl_2 (v:v = 1:3) was refluxed for 12 h. The solvent was rotoevaporated, and the residues were chromatographed on a silica gel column to purify Ir−COOH. The mixture of CH_2Cl_2 and *n*-hexane (v/v = 5/1) was first used as eluent to remove the small polar impurities, and then CH_2Cl_2/methane (v/v = 3/1) was employed to gain purified Ir−COOH. ^{1}H NMR (DMSO-d_6, 400 MHz), ppm: 8.83 (1H), 8.75 (1H), 8.25 (m, 2H), 7.90 (m, 4H), 7.69−7.56 (m, 4H), 7.50 (m, 2H), 7.21−7.13 (m, 2H), 6.99 (m, 2H), 6.88 (tt, J = 7.6, 1.2 Hz, 2H), 6.19 (dt, J = 7.6, 1.2 Hz, 2H), 3.16 (s, 1H), 2.75 (t, *J* = 7.2 Hz, 2H), 2.52 (s, 3H), 1.89−1.76 (m, 4H). *m*/*z* (TOF-MS, solvent: methyl alcohol), 757.2, corresponding to $[C_{37}H_{32}IrN_4O_2]^+$. Anal. Calcd for $C_{37}H_{32}IrN_4O_2Cl$: C, 56.09; H, 4.07; N, 7.07. Found: C, 56.01; H, 4.24; N, 7.01.

Step 3, 1 equiv of Ir−COOH was added to a DMF solution of 1 equiv of NHS and 1.2 equiv of HBTU. The mixture was stirred for 12 h under an argon atmosphere at room temperature. The solvent was rotoevaporated, and the residues were chromatographed on a silica gel column to purify Ir−NHS. The mixture of CH_2Cl_2 and *n*-hexane (v/v = 5/1) was first used as eluent to remove the small polar impurities, and then CH_2Cl_2/methane (v/v = 2/1) was employed to gain purified Ir−NHS. ^{1}H NMR (DMSO-d_6, 400 MHz), ppm: 8.77 (m, 2H), 8.26 (d, *J* = 8.4 Hz, 2H), 7.93 (m, 4H), 7.76−7.50 (m, 6H), 7.16 (m, 2H), 7.02 (t, *J* = 7.6 Hz, 2H), 6.90 (t, *J* = 7.2 Hz, 2H), 6.20 (t, *J* = 7.2 Hz, 2H), 2.96−2.68 (m, 8H), 2.54 (s, 3H), 2.00 (m, 2H). *m*/*z* (TOF-MS, solvent: methyl alcohol), 854.2, corresponding to $[C_{41}H_{35}IrN_5O_4]^+$. Anal. Calcd for $C_{41}H_{35}IrN_5O_4Cl$: C, 55.37; H, 3.97; N, 7.87. Found: C, 54.91; H, 4.29; N, 7.82.

Performance of DNA Detection in HEPES Buffer. GO nanosheets were synthesized according to our previously reported procedure of a modified Hummer's method.[29] The Ir-ssDNA probe with a sequence of 5′-Ir complex-ACG-CATCTGTGAAGAGAACCTGGG-3′ was synthesized and purified by Takara (Dalian, China). FAM-labeled ssDNA (FAM-ssDNA) probe was prepared and purified as control under similar reaction conditions. Other DNA oligonucleotides used in this work were synthesized by Shanghai Sangon Biotechnology Co., Ltd. (Shanghai, China). The sequences of oligonucleotides are given in Table 1. The HEPES buffer consisted of 20 mM HEPES (pH 7.6), 150 mM NaCl, and 1 mM $MgCl_2$.[30] Milli-Q (resistance = 18.2 MΩ cm) purified water was used in all of the solutions.

Table 1. Synthesized Oligonucleotide Sequences (5′→3′) Used in the Experiments

DNA	sequence (5′→3′)
probe	ACGCATCTGTGAAGAGAACCTGGG
target	CCCAGGTTCTCTTCACAGATGCGT
single base mismatch 1	CCCAGGTTCTATTCACAGATGCGT
single base mismatch 2	CCCAGGTTCTTTTCACAGATGCGT
two base mismatch	CCCAGGTTCTGTTCAAAGATGCGT
scramble DNA	TCCCATCTGAGATGAGAAGCTGGG

DOI: 10.1021/acs.analchem.5b04324
Anal. Chem. 2016, 88, 1892−1899

Scheme 1. Chemical Structures and the Synthetic Route to the Iridium(III) Complexes[a]

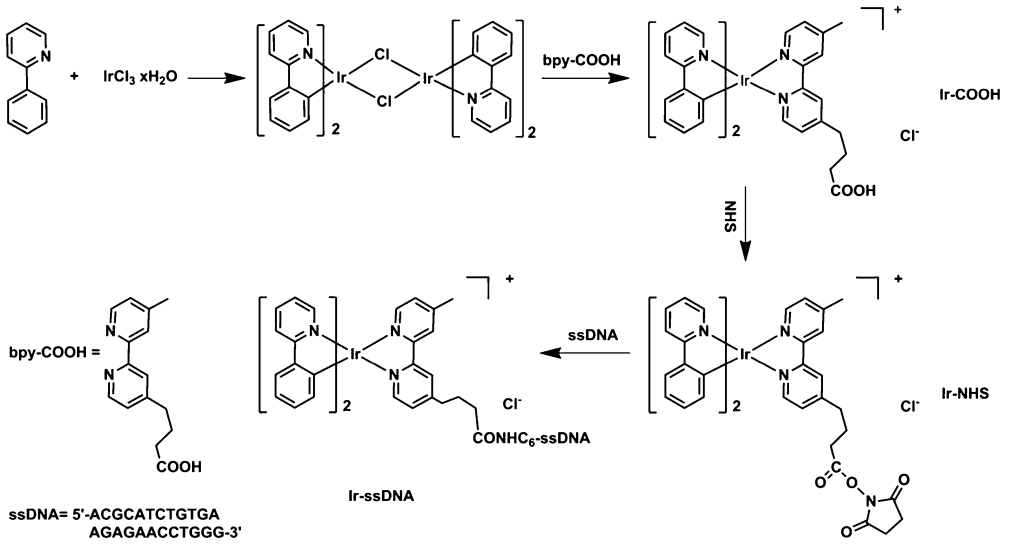

[a]Step 1, 2-ethoxyethanol/H_2O, reflux; Step 2, CH_3OH/CH_2Cl_2, reflux; Step 3, HBTU, DMF, Ar gas, room temperature; Step 4, DMSO/H_2O, room temperature.

For the luminescence emission spectra analysis, 30 μg/mL GO and 20 nM Ir-ssDNA probe were mixed together in HEPES buffer, and then different concentrations of the target DNA were added into the solution. After this mixture was allowed to bind for about 30 min at 37 °C, the luminescence of the mixture was detected. All of the experiments were accomplished in an opening environment without any extra shielding devices.

Photostability Comparison of Ir Complex and FAM. To guarantee reliable comparison, the luminescence intensities of Ir complex and FAM were adjusted to the same value. The two samples were continuously irradiated for different time intervals using a 100 W xenon lamp of 365 nm.

Photostability Comparison of GO-Ir-ssDNA and GO-FAM-ssDNA Biosensors. For the photostability comparison experiment, 20 μg/mL GO and 20 nM of the Ir complex/FAM-labeled ssDNA were mixed together, then the samples were continuously irradiated for different time intervals using a UV lamp, after irradiation, 20 nM fully complementary target DNA was added to the solution incubating for 30 min at 37 °C, and, at last, the luminescence of the solution was detected.

RESULTS AND DISCUSSION

Synthesis of Ir Complexes and Ir-ssDNA. The chemical structures of the iridium(III) complexes and their general synthetic routes are shown in Scheme 1. Ir complex with carboxyl group was synthesized with bpy-COOH as ancillary ligand, followed by reacting with NHS. The NHS-activated Ir complex was further tagged onto the amino terminate of ssDNA for DNA detection. Their chemical structures were characterized by TOF-MS (Figure 1). The mass spectra of Ir complexes with COOH and NHS groups featured a major peak centered at m/z 757.2 and 853.7, respectively, which were in accord with the theoretically calculated values. As illustrated in Figure 1c, as compared to the m/z of ssDNA centered at 7426.9, m/z of Ir-ssDNA was increased to 8332.1, contributed by the Ir complex modification. Additionally, the photophysical properties of Ir complexes were also investigated. The UV/vis absorption spectra of Ir complexes in methyl alcohol are shown in Figure 2a; both iridium(III) complexes exhibited very strong intraligand absorption bands ($\pi-\pi^*$) in the range of 250−300 nm ($\varepsilon > 10\,000\ M^{-1}\ cm^{-1}$) and weaker MLCT transition bands from 350 to 450 nm, which was similar to the previous report about other heteroleptic iridium(III) complexes.[31,32] Figure 2b represents the luminescence emission spectra of the iridium-(III) complexes. Their emission peaks were localized at 570 nm, and no obvious difference was observed. The linear phosphorescence quantum yields of Ir complexes with COOH and NHS groups were 16% and 18%, and their emission lifetimes were 0.48 and 0.24 μs (Figure S3).

Interaction between Ir Complex and GO. The interaction between Ir complex and GO was investigated via measurements upon mixing the luminescent complex and the as-prepared GO nanosheets. We first characterized the GO sample to confirm their exfoliation. The chemically synthesized GO showed excellent water-dispersible due to the presence of oxygen-containing functional groups on the surface; tapping-mode AFM measurement revealed that the thickness of GO was 1.3 nm, characteristic of a fully exfoliated GO sheet (Figure S4).[29] The luminescence quenching ability of GO toward the Ir complex was further measured to evaluate the feasibility of fabrication of GO−Ir-based biosensors. As depicted in Figure 3a, the luminescence intensity of Ir complex decayed significantly with the addition of GO nanosheets. A sharp decrease in luminescence intensity occurred over GO concentrations ranging from 0 to 30 μg/mL, and the luminescence of Ir complex (20 nM) was almost quenched when the GO concentration was up to 30 μg/mL.

Meanwhile, the influence of GO on the luminescence intensity of Ir complex was studied. Figure 3b plots the luminescence intensity of Ir complex and Ir−GO mixture as a function of Ir complex concentration. It can be seen that the luminescence intensity of Ir complex and Ir−GO mixture increased linearly with an increase of GO concentration from 0 to 20 μg/mL. The intensities of Ir−GO mixture were tremendously lower than those of free Ir complex. This result demonstrated Ir complex as a luminescence probe can be effectively quenched by GO nanosheets. The quenching

DOI: 10.1021/acs.analchem.5b04324
Anal. Chem. 2016, 88, 1892−1899

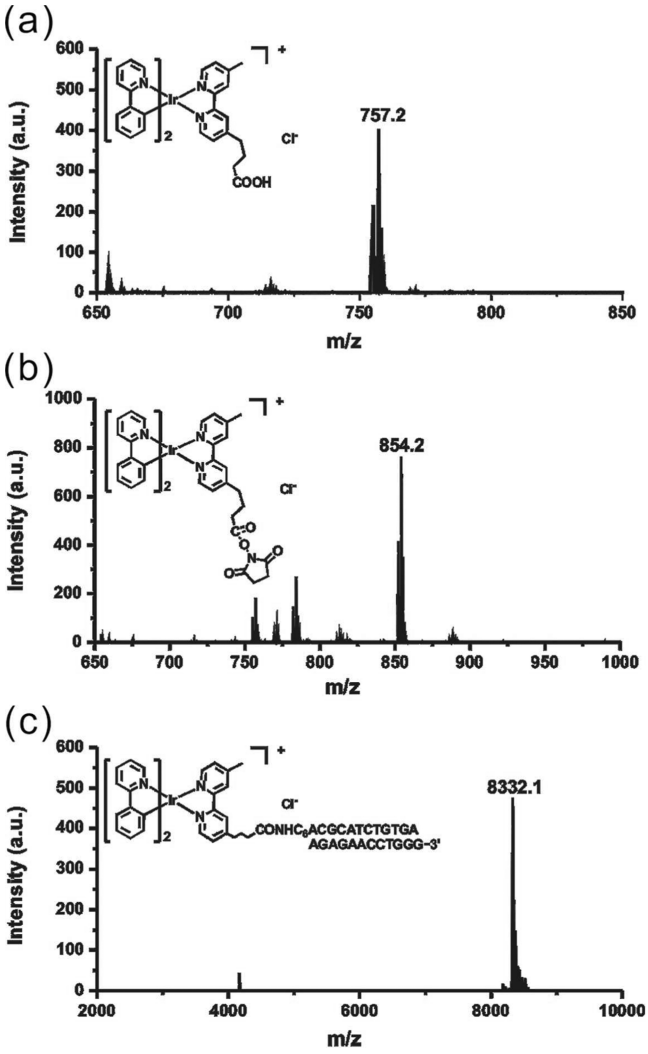

Figure 1. Mass spectra of Ir complex (with carboxyl group) (a), NHS activated (b), and Ir-ssDNA (c, DNA sequence, 5′-ACGCATCTGT-GAAGAGAACCTGGG-3′). The insets illustrate their corresponding molecular structures.

procedure of Ir complex with GO is illustrated in the inset of Figure 3a. When the Ir complex mixes with GO, Ir complex can be strongly adsorbed on the surface of the GO plane due to $\pi-\pi$ stacking[29] and electrostatic attraction force[33] between Ir complex and carbon nanosheets (see Figure S5 for a detailed discussion). Consequently, the luminescence of Ir complex is quenched on the basis of the highly efficient long-range energy transfer from Ir complex to GO.[14,34]

Design Strategy. The strong FRET effect between Ir and GO makes GO an effective platform for the development of GO−Ir-based luminescence biosensor. Figure 4 illustrates the sensing strategy for the detection of target DNA. In the absence of target, Ir-ssDNA probe can be adsorbed onto GO nanosheet by $\pi-\pi$ stacking between Ir-ssDNA and sp^2-bonded graphene, bringing the Ir-ssDNA into close proximity with the GO plane. Consequently, the luminescence of Ir complex is quenched via FRET from Ir complex to GO. In the presence of target DNA, probe ssDNA specifically hybridizes with target ssDNA. The formed dsDNA helix possesses weak binding affinity to the graphene surface, leading to release of dsDNA from GO surface. Simultaneously, the Ir complex is also pulled away from the graphene surface; as a result, the luminescence of the Ir

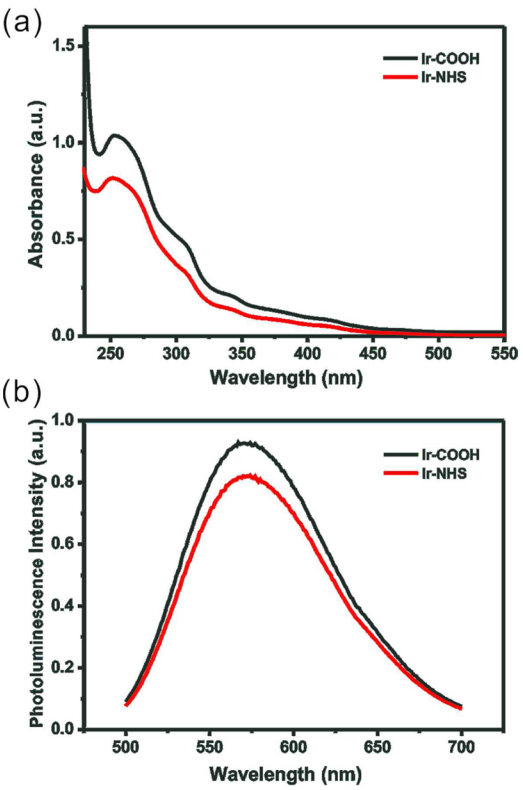

Figure 2. Absorption (a) and normalized emission (b) spectra of Ir complexes in methyl alcohol solutions (20 μM, λ_{ex} = 360 nm).

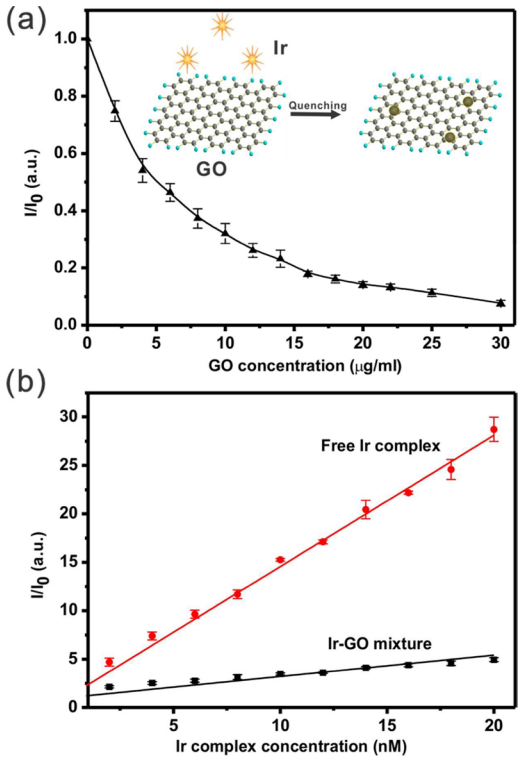

Figure 3. (a) Photoluminescence intensity of the mixture of Ir complex as a function of GO concentration. Inset depicts the process of Ir complex quenched by GO. (b) The intensities of Ir complex and Ir−GO mixture (GO, 20 μg/mL) as a function of Ir complex concentration.

DOI: 10.1021/acs.analchem.5b04324
Anal. Chem. 2016, 88, 1892−1899

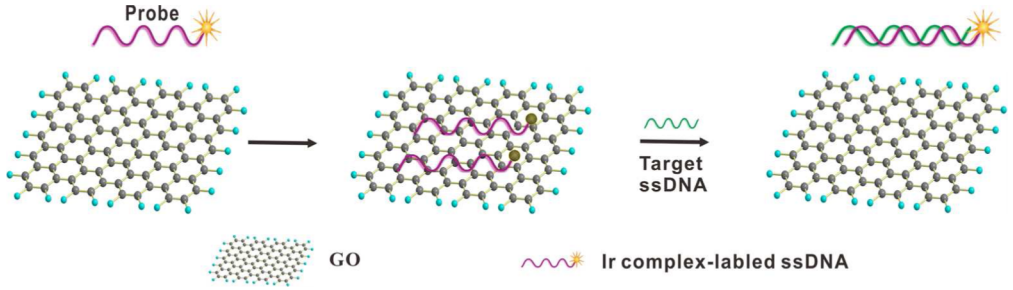

Figure 4. Scheme for the mechanism of GO-based biosensor for the DNA detection.

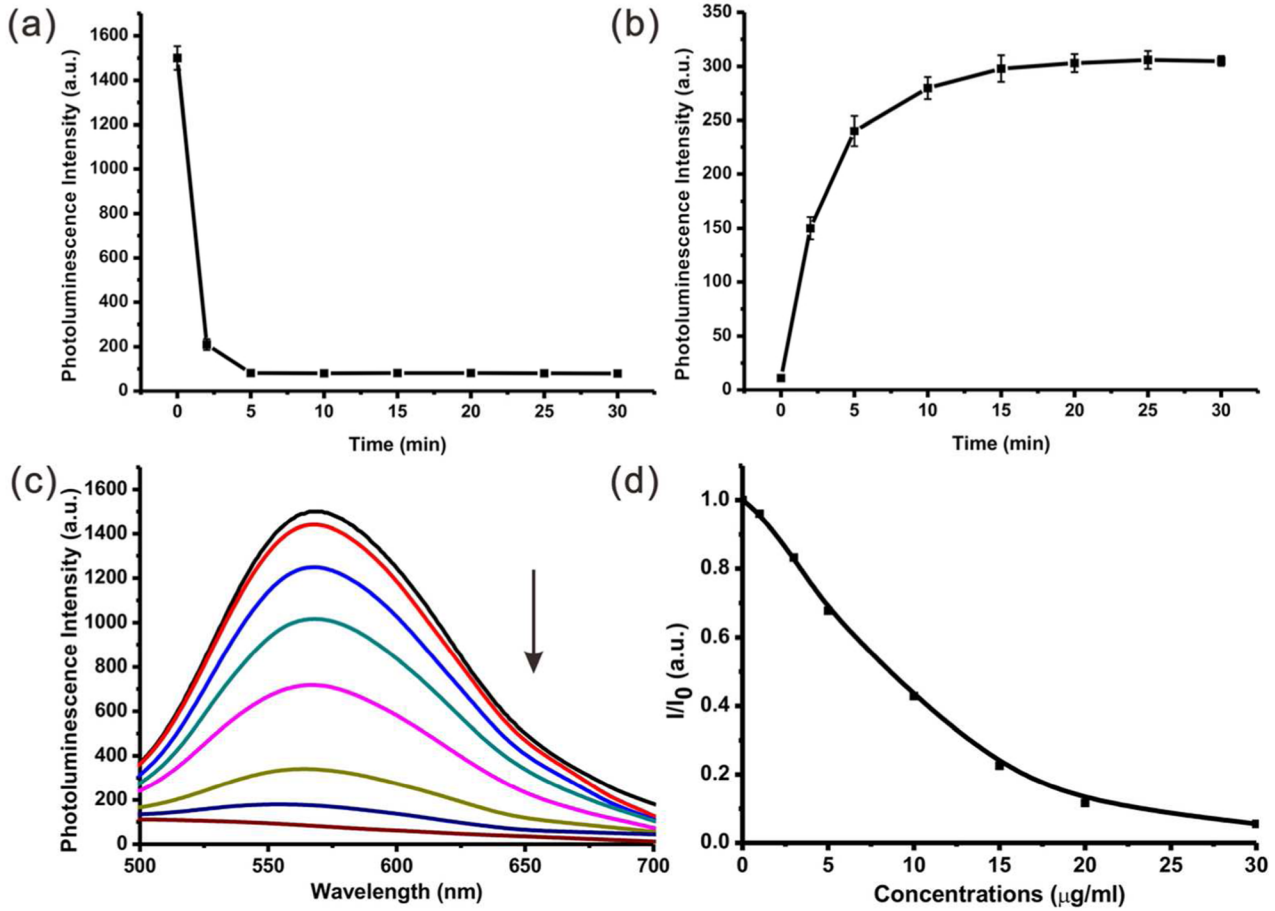

Figure 5. (a) Luminescence of Ir-ssDNA (20 nM) in HEPES buffer quenched by GO as a function of reaction time. (b) Luminescence intensity versus different reaction time of GO-Ir-ssDNA biosensor (20 nM of Ir-ssDNA) with target DNA (20 nM). (c) Luminescence quenching spectra and normalized intensity (d) of Ir-ssDNA (20 nM) in the absence (black) and presence of GO with a series of concentrations.

complex gets recovered. The high quenching efficiency of GO toward Ir complex offers a high signal-to-background ratio, and thus high sensitivity for target DNA detection can be accomplished. Hence, a platform for sensitive detection of biomolecules could be constructed by using GO and Ir complex as the FRET pair.

To unravel the optimal reaction time between Ir-ssDNA and GO, and the optimal time between GO-Ir-ssDNA and target DNA, the kinetic behaviors of Ir-ssDNA and GO, as well as GO-Ir-ssDNA with target DNA, were evaluated by monitoring the luminescence intensity as a function of reaction time. Figure 5a shows the luminescence quenching of Ir-ssDNA in the presence of GO as a function of incubation time. It can be observed that Ir-ssDNA adsorption on the surface of graphene was very fast at room temperature. It reached equilibrium within 5 min. In addition, Figure 5b depicts luminescence intensity versus different reaction time of GO-Ir-ssDNA biosensor (20 nM) with target DNA (20 nM). It was indicated that the formation and release of the dsDNA helix from GO were relatively slow and completed in about 30 min at 37 °C.

Moreover, the luminescence quenching behavior of Ir-ssDNA with GO was evaluated to estimate the optimal concentration of GO. As shown in Figure 5c and d, luminescence intensity of Ir-ssDNA (20 nM) declined sharply as the concentration of GO increased from 0 to 30 μg/mL. When the concentration of GO was up to 30 μg/mL, the luminescence intensity of Ir complex was quenched down to 5% of original signal. Thus, 30 μg/mL of GO was taken as the optimized concentration for the preparation of GO-Ir-ssDNA biosensor.

DOI: 10.1021/acs.analchem.5b04324
Anal. Chem. 2016, 88, 1892−1899

Target Detection and Specificity of GO-Ir-ssDNA Biosensor. After we successfully optimized the experimental conditions, we used this GO-Ir-ssDNA biosensor for DNA detection. Figure 6a shows the luminescence emission spectra

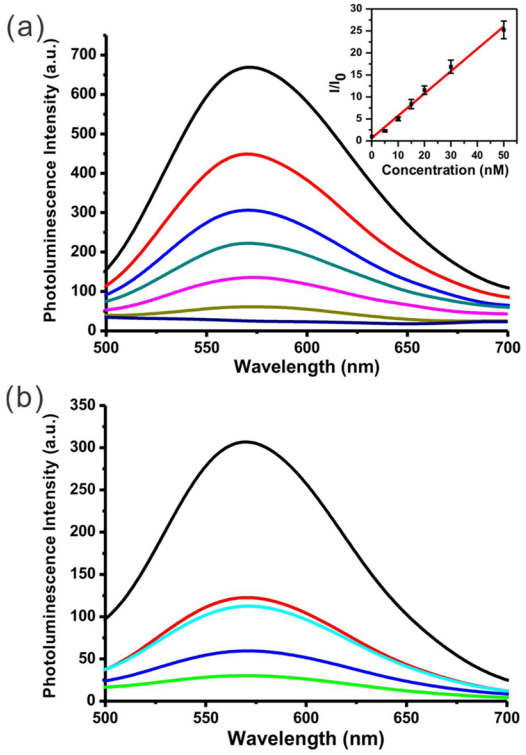

Figure 6. (a) Typical luminescence emission spectra for GO-Ir-ssDNA biosensor (20 nM) in the presence of various concentrations of target DNA (0, 5, 10, 15, 20, 30, and 50 nM). The inset plots linear fitting curve for the luminescence intensity versus the target DNA concentration. (b) Luminescence response spectra for the GO-Ir-DNA biosensor (20 nM) in the presence of 20 nM of the fully complementary target T1 (black), single-base mismatched target M1 (red), M2 (cyan), two-base mismatched target M3 (blue), and scrambled DNA S1 (green).

of biosensor in the presence of different concentrations of target DNA. The luminescence intensity of the biosensor dramatically increased with increasing concentration of target DNA from 5 to 50 nM. The calibration curve for target DNA detection is represented in the inset of Figure 6a, and the linear range was from 5 to 50 nM with a linear equation of $y = 30.828x + 38.15$ (regression coefficient $R^2 = 0.9901$), where y is the ratio of I/I_0 (I_0 and I are the luminescence intensities of Ir-ssDNA at 570 nm in the absence and presence of target DNA, respectively), and x denotes the concentration of target DNA. The above-mentioned experimental results demonstrated that this GO-based biosensor can be used as a sensitive approach for DNA detection.

To investigate the specificity of GO-Ir-ssDNA biosensor, we compared the luminescence response induced by DNA strands containing single-base and two-base-mismatched oligonucleotides with that of target DNA (Table 1). All of the results are displayed in Figure 6b. It was found that the luminescence signal for fully complementary target T1 was approximately 2.5 and 5 times higher than those for the single-base mismatched and two-base mismatched targets, respectively. Notably, minimal luminescence increase was acquired in the presence of scramble DNA.[35] These results revealed that this GO-Ir-ssDNA biosensor can be used to discriminate perfectly matched and mismatched DNA targets, making it a promising platform for sensitive and selective DNA detection.

Photostability Comparison of Ir Complex, FAM, and Their Biosensors. Because the photostability of dye and dye-based biosensor plays a crucial role in their usage, storage, and lifetime, Ir complex and GO-Ir-ssDNA are irradiated under rigorous UV condition with FAM and FAM-based biosensor as control to evaluate their photostability.[36] Figure 7a illustrated

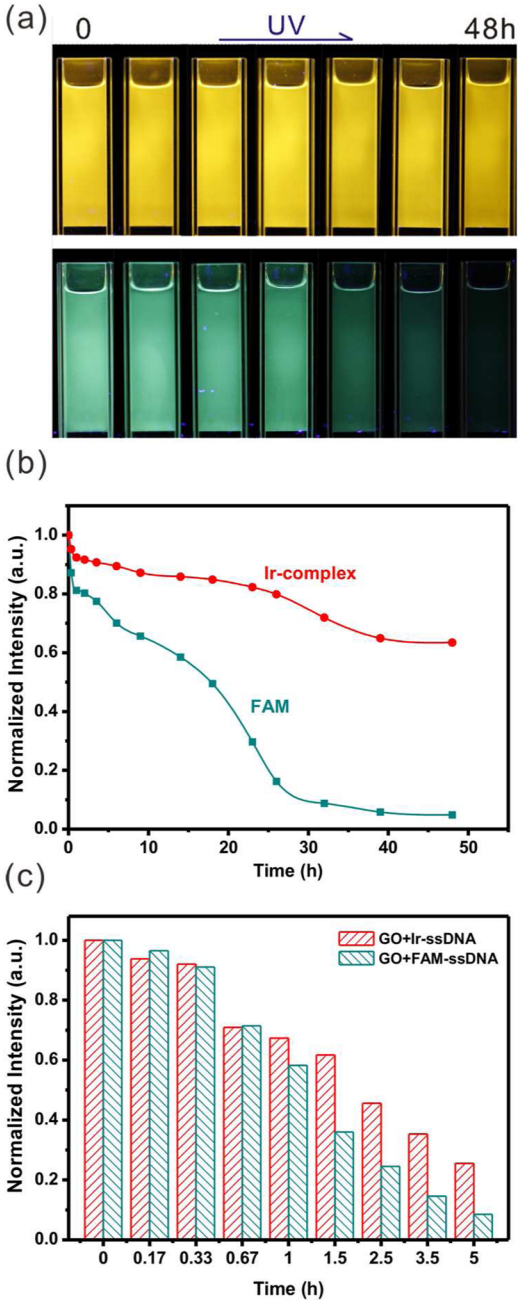

Figure 7. Temporal evolution of luminescence decay of free Ir complex, FAM, and their biosensors irradiated by UV light (365 nm, 100 W). (a) Digital photographs and (b) the intensity decay curves of Ir complex and FAM. (c) Normalized luminescence intensity of biosensors (20 nM) as a function of irradiation time, followed by recovery with 20 nM target ssDNA.

DOI: 10.1021/acs.analchem.5b04324
Anal. Chem. 2016, 88, 1892−1899

the photographs of Ir complex and FAM under UV irradiation. Both samples exhibited distinct luminescence during initial UV irradiation. The fluorescent signal of the FAM image was constantly reduced with increasing irradiation time and almost completely diminished after 48 h irradiation, whereas the Ir complex preserved stable and bright luminescence during long time (e.g., 48 h) irradiation under the same experiment conditions. Figure 7b plots temporal evolution of luminescence intensity decay of Ir complex and FAM. It was found that the luminescence of FAM was quickly decreased to 80% in 2 h, and as time progressed, the intensity decreased to 16% in 26 h, and after 48 h irradiation, the luminescence was only 4.8%. In contrast, the luminescence intensity of the Ir complex was extremely stable, preserving ~83% of the initial intensity after 20 h irradiation; in the following time, the luminescence decreased slowly and preserved 63.5% after 48 h irradiation. This result proved that, as compared to traditional FAM dye, Ir complex possessed remarkable photostability.

Subsequently, the photostability of GO-Ir-ssDNA was measured with GO-FAM-ssDNA biosensor as control. GO-Ir-ssDNA (20 nM) and GO-FAM-ssDNA (20 nM) biosensors were simultaneously irradiated by UV lamp for a certain duration, then 20 nM fully complementary ssDNA was added, and after incubation at 37 °C for 30 min, their luminescence intensities were detected. As shown in Figure 7c, for the initial 40 min, the restored luminescence intensity of both GO-Ir-ssDNA and GO-FAM-ssDNA biosensors decayed nearly at a similar percentage of initial value, whereas after 1 h of UV irradiation, the restored intensity of GO-Ir-ssDNA biosensor was discriminable higher than that of GO-FAM-ssDNA biosensor. Finally, after 5 h of irradiation, only about 8.5% of fluorescence intensity was recovered for GO-FAM-ssDNA biosensor. In contrast, the fluorescence intensity recovery of GO-Ir-ssDNA biosensor was about 25.5%, nearly 3 times higher than that of traditional fluorescent dye. The difference in luminescence decay behavior between the free dyes and biosensors should be mainly ascribed to the photostability of GO and DNA sequence. In the sensing system, GO can be partially reduced under fierce UV irradiation. For the reduced GO that possesses higher absorbance performance than the initial GO,[37] the partially reduced GO can absorb a portion of the recovered luminescence, leading to a decrease in luminescence intensity for the biosensors. On the other hand, under continuous UV irradiation, ssDNA structure is damaged.[38] Because the affinity between the degraded ssDNA and the target shrunk, the degraded dye-ssDNA can hardly hybridize with target DNA to form a duplex structure, causing a loss of luminescence intensity recovery. Although the luminescence recovery is encumbered by the unstable GO and DNA sequence, it is still safe to conclude that the GO-Ir-ssDNA biosensor possesses better photostability than the GO-FAM-ssDNA biosensor, which is inherited from the highly photostable Ir complex. Furthermore, it is worth noting that due to the high photostability, all of the DNA detection experiments using GO-Ir-ssDNA biosensor can be carried out in an opening environment without extra shielding device. This unique property enabled the GO-Ir-based biosensor as more reliable and ease of use for biomolecule detection, offering a new opportunity to construct a long-life biosensor for molecular diagnostics,[39] genomic research, and drug development.[40]

CONCLUSION

In summary, iridium(III) complex with carboxyl group was successfully synthesized, activated with NHS, and further labeled on the amino terminal of ssDNA. After introducing Ir-ssDNA into the GO-based biosensing system, we demonstrated the applicability of the luminescent complex as a fast, sensitive, and selective luminescence probe in target DNA detection. More interestingly, the GO-Ir-ssDNA biosensor exhibited excellent photostability as compared to the traditional organic dye FAM-labeled biosensor, which was inherited from the ultrahighly photostable Ir complex. It can be anticipated that the Ir complexes combined with their excellent biocompatibility and extraordinary photostability will impart potential use for DNA detection, making them promising for applications in the field of genomic research and drug development.

ASSOCIATED CONTENT

Supporting Information

The Supporting Information is available free of charge on the ACS Publications website at DOI: 10.1021/acs.analchem.5b04324.

Supplementary figures, ^{1}H NMR spectra, quantum yields and lifetimes of Ir complexes, AFM image of GO, and Ir complex/FAM loading and release behaviors (PDF)

AUTHOR INFORMATION

Corresponding Authors

*E-mail: qzhang2012@suda.edu.cn.
*E-mail: jliu@suda.edu.cn.

Author Contributions

§Qing.Z. and Y.Z. contributed equally to this work.

Notes

The authors declare no competing financial interest.

ACKNOWLEDGMENTS

This work was supported by the National Natural Science Foundation of China (NSFC nos. 31400806, 21505097, 11204349), NSF of Jiangsu Province (BK20130306, BK20150283), and the University Scientific Research Project of Jiangsu Province (15KJB150027). We thank Dr. Ruigong Su for helpful discussions.

REFERENCES

(1) Velusamy, V.; Arshak, K.; Korostynska, O.; Oliwa, K.; Adley, C. *Biotechnol. Adv.* **2010**, *28*, 232−254.
(2) Rosi, N. L.; Mirkin, C. A. *Chem. Rev.* **2005**, *105*, 1547−1562.
(3) Giljohann, D. A.; Seferos, D. S.; Daniel, W. L.; Massich, M. D.; Patel, P. C.; Mirkin, C. A. *Angew. Chem., Int. Ed.* **2010**, *49*, 3280−3294.
(4) Gill, R.; Zayats, M.; Willner, I. *Angew. Chem., Int. Ed.* **2008**, *47*, 7602−7625.
(5) Kim, S. N.; Rusling, J. F.; Papadimitrakopoulos, F. *Adv. Mater.* **2007**, *19*, 3214−3228.
(6) Zhu, C.; Zeng, Z.; Li, H.; Li, F.; Fan, C.; Zhang, H. *J. Am. Chem. Soc.* **2013**, *135*, 5998−6001.
(7) He, Y.; Wang, Z.-G.; Tang, H.-W.; Pang, D.-W. *Biosens. Bioelectron.* **2011**, *29*, 76−81.
(8) He, Y.; Lin, Y.; Tang, H.; Pang, D. *Nanoscale* **2012**, *4*, 2054−2059.
(9) Zhao, X.-H.; Kong, R.-M.; Zhang, X.-B.; Meng, H.-M.; Liu, W.-N.; Tan, W.; Shen, G.-L.; Yu, R.-Q. *Anal. Chem.* **2011**, *83*, 5062−5066.
(10) Wang, Y.; Li, Z.; Hu, D.; Lin, C.-T.; Li, J.; Lin, Y. *J. Am. Chem. Soc.* **2010**, *132*, 9274−9276.

DOI: 10.1021/acs.analchem.5b04324
Anal. Chem. 2016, 88, 1892−1899

(11) Xing, X.-J.; Xiao, W.-L.; Liu, X.-G.; Zhou, Y.; Pang, D.-W.; Tang, H.-W. *Biosens. Bioelectron.* **2016**, *78*, 431−437.
(12) Liu, Z.; Robinson, J. T.; Sun, X.; Dai, H. *J. Am. Chem. Soc.* **2008**, *130*, 10876−10877.
(13) Xu, H.; Yang, Q.; Li, F.; Tang, L.; Gao, S.; Jiang, B.; Zhao, X.; Wang, L.; Fan, C. *Analyst* **2013**, *138*, 2678−2682.
(14) Swathi, R. S.; Sebastian, K. L. *J. Chem. Phys.* **2008**, *129*, 054703.
(15) Tang, Z.; Wu, H.; Cort, J. R.; Buchko, G. W.; Zhang, Y.; Shao, Y.; Aksay, I. A.; Liu, J.; Lin, Y. *Small* **2010**, *6*, 1205−1209.
(16) Yang, X.; Niu, G.; Cao, X.; Wen, Y.; Xiang, R.; Duan, H.; Chen, Y. *J. Mater. Chem.* **2012**, *22*, 6649−6654.
(17) Lu, C.-H.; Yang, H.-H.; Zhu, C.-L.; Chen, X.; Chen, G.-N. *Angew. Chem.* **2009**, *121*, 4879−4881.
(18) He, S.; Song, B.; Li, D.; Zhu, C.; Qi, W.; Wen, Y.; Wang, L.; Song, S.; Fang, H.; Fan, C. *Adv. Funct. Mater.* **2010**, *20*, 453−459.
(19) Li, C.; Yu, M.; Sun, Y.; Wu, Y.; Huang, C.; Li, F. *J. Am. Chem. Soc.* **2011**, *133*, 11231−11239.
(20) Zhou, Y.; Jia, J.; Li, W.; Fei, H.; Zhou, M. *Chem. Commun.* **2013**, *49*, 3230−3232.
(21) Ivanov, P.; O'Day, E.; Emara, M. M.; Wagner, G.; Lieberman, J.; Anderson, P. *Proc. Natl. Acad. Sci. U. S. A.* **2014**, *111*, 18201−18206.
(22) Leung, K.-H.; He, H.-Z.; He, B.; Zhong, H.-J.; Lin, S.; Wang, Y.-T.; Ma, D.-L.; Leung, C.-H. *Chem. Sci.* **2015**, *6*, 2166−2171.
(23) Lin, S.; Gao, W.; Tian, Z.; Yang, C.; Lu, L.; Mergny, J.-L.; Leung, C.-H.; Ma, D.-L. *Chem. Sci.* **2015**, *6*, 4284−4290.
(24) Yu, M.; Zhao, Q.; Shi, L.; Li, F.; Zhou, Z.; Yang, H.; Yi, T.; Huang, C. *Chem. Commun.* **2008**, 2115−2117.
(25) Zhao, Q.; Li, F.; Huang, C. *Chem. Soc. Rev.* **2010**, *39*, 3007−3030.
(26) Amao, Y.; Ishikawa, Y.; Okura, I. *Anal. Chim. Acta* **2001**, *445*, 177−182.
(27) Schmid, B.; Garces, F. O.; Watts, R. J. *Inorg. Chem.* **1994**, *33*, 9−14.
(28) Tan, W.; Zhang, Q.; Zhang, J.; Tian, H. *Org. Lett.* **2009**, *11*, 161−164.
(29) Zhang, Q.; Li, W.; Kong, T.; Su, R.; Li, N.; Song, Q.; Tang, M.; Liu, L.; Cheng, G. *Carbon* **2013**, *51*, 164−172.
(30) Huang, P.-J. J.; Liu, J. *Anal. Chem.* **2012**, *84*, 4192−4198.
(31) Sajoto, T.; Djurovich, P. I.; Tamayo, A.; Yousufuddin, M.; Bau, R.; Thompson, M. E.; Holmes, R. J.; Forrest, S. R. *Inorg. Chem.* **2005**, *44*, 7992−8003.
(32) Yang, C.-H.; Cheng, Y.-M.; Chi, Y.; Hsu, C.-J.; Fang, F.-C.; Wong, K.-T.; Chou, P.-T.; Chang, C.-H.; Tsai, M.-H.; Wu, C.-C. *Angew. Chem.* **2007**, *119*, 2470−2473.
(33) Park, S.; Lee, K.; Bozoklu, G.; Cai, W.; Nguyen, S.; Ruoff, R. *ACS Nano* **2008**, *2*, 572−578.
(34) Dong, H.; Gao, W.; Yan, F.; Ji, H.; Ju, H. *Anal. Chem.* **2010**, *82*, 5511−5517.
(35) Zhao, X.-H.; Ma, Q.-J.; Wu, X.-X.; Zhu, X. *Anal. Chim. Acta* **2012**, *727*, 67−70.
(36) Zhong, Y.; Peng, F.; Bao, F.; Wang, S.; Ji, X.; Yang, L.; Su, Y.; Lee, S.-T.; He, Y. *J. Am. Chem. Soc.* **2013**, *135*, 8350−8356.
(37) Li, D.; Muller, M. B.; Gilje, S.; Kaner, R. B.; Wallace, G. G. *Nat. Nanotechnol.* **2008**, *3*, 101−105.
(38) Sinha, R. P.; Hader, D.-P. *Photochem. Photobiol. Sci.* **2002**, *1*, 225−236.
(39) Zhong, H.-J.; Lu, L.; Leung, K.-H.; Wong, C. C. L.; Peng, C.; Yan, S.-C.; Ma, D.-L.; Cai, Z.; David Wang, H.-M.; Leung, C.-H. *Chem. Sci.* **2015**, *6*, 5400−5408.
(40) Wang, Y.; Li, Z.; Wang, J.; Li, J.; Lin, Y. *Trends Biotechnol.* **2011**, *29*, 205−212.

DOI: 10.1021/acs.analchem.5b04324
Anal. Chem. 2016, 88, 1892−1899